

Autoencoder Based Sample Selection for Self-Taught Learning

Siwei Feng, *Student Member, IEEE*, and Marco F. Duarte, *Senior Member, IEEE*

Abstract—Self-taught learning is a technique that uses a large number of unlabeled data as source samples to improve the task performance on target samples. Compared with other transfer learning techniques, self-taught learning can be applied to a broader set of scenarios due to the loose restrictions on source data. However, knowledge transferred from source samples that are not sufficiently related to the target domain may negatively influence the target learner, which is referred to as negative transfer. In this paper, we propose a metric for the relevance between a source sample and target samples. To be more specific, both source and target samples are reconstructed through a single-layer autoencoder with a linear relationship between source samples and target samples simultaneously enforced. An $\ell_{2,1}$ -norm sparsity constraint is imposed on the transformation matrix to identify source samples relevant to the target domain. Source domain samples that are deemed relevant are assigned pseudo-labels reflecting their relevance to target domain samples, and are combined with target samples in order to provide an expanded training set for classifier training. Local data structures are also preserved during source sample selection through spectral graph analysis. Promising results in extensive experiments show the advantages of the proposed approach.

Index Terms—Self-Taught Learning, Sample Selection, Autoencoder, $\ell_{2,1}$ -Norm Sparsity, Spectral Graph Analysis.

1 INTRODUCTION

SUPERVISED learning has excelled in many machine learning tasks such as classification [1, 2] and regression [3, 4]. However, the success of a supervised learning algorithm requires large-scale labeled training datasets and that both training and testing data sharing the same label and feature space.¹ These conditions limit the applications of supervised learning methods in practical scenarios since it is expensive to collect eligible training data [5, 6].

Several techniques have been proposed to tackle the limitations of supervised learning methods. Semi-supervised learning [7–9] algorithms use both labeled and unlabeled data to improve performance when labeled training data are limited. However, many semi-supervised learning algorithms assume that unlabeled data and labeled data have the same distribution [7, 8] or class labels [9]. The success of semi-supervised learning highly depends on the validity of these assumptions. However, it is still difficult to gather unlabeled data which satisfy these preconditions.

In order to further loosen the restrictions on training data, many transfer learning approaches [10, 11] have been proposed. Transfer learning methods use the knowledge obtained from a source domain to improve the performance on target domain tasks. Self-taught learning [12–20] is the type of transfer learning techniques most similar to semi-supervised learning, which also employs unlabeled data with the attempt to improve supervised learning performance when labeled training data are limited. However, compared with semi-supervised learning, self-taught learning methods have fewer restrictions on unlabeled data,

as they allow the label spaces and marginal probability distributions of unlabeled and labeled data to be different. In self-taught learning, unlabeled data are used as source from which the knowledge learned is applied to tasks performed on labeled target data. Such a loose restriction on unlabeled data significantly simplifies learning due to the huge volume of unlabeled data we can access. However, the easily obtained unlabeled data inevitably contain samples with weak relation to the labeled training data, which may even harm the supervised learning performance if we treat them equally as other unlabeled samples during knowledge transfer. This is known as negative transfer. Therefore, it is necessary to select samples that are related to the labeled data to reduce the impact caused by negative transfer.

In this paper, we propose a novel algorithm for self-taught learning with unlabeled source data which are related to labeled target data to be selected. The algorithm leverages a linear mapping, a k -nearest neighbor (k NN) graph and a single-layer autoencoder to obtain a metric for cross domain relevance. We refer to this method as graph and autoencoder-based self-taught learning (GASTL). The framework of GASTL includes two modules: a source sample re-weighting module and a classifier training module. In the first module, we assign each unlabeled source sample a weight that indicates its relevance to labeled target samples.² In the second module, source samples with large weights are selected to combine a training set with target data to train a classifier. Each selected source sample is assigned a pseudo-label from the target domain label space to be used during classifier training. The weights of source samples are also used during classifier training. The trained

• The authors are with the Department of Electrical and Computer Engineering, University of Massachusetts, Amherst, MA 01003 USA (e-mail: siwei@engin.umass.edu; mduarte@ecs.umass.edu).

1. “Training data” is used in the sequel to denote data used for model learning.

2. The setting of self-taught learning requires source samples to be unlabeled and target samples to be labeled. Therefore in the sequel we do not specify the availability of label information for both source and target samples.

classifier is then used to predict labels of unseen target samples.

The key contributions of this paper are as follows:

- We propose a novel metric for the relevance of each source sample to the target domain in the scenario of self-taught learning based on an autoencoder and graph data regularization. To the best of our knowledge, we are the first to measure source and target sample relevance for self-taught learning problems.
- We propose a novel classifier training scheme with both selected source samples and target samples as training dataset with the relevance of each source sample to target domain being considered. We are not aware of existing self-taught learning approaches that integrate cross domain relevance into classifier training.
- We present an efficient solver for the knowledge transfer optimization problem described above that relies on an iterative scheme based on the gradient descent of the proposed objective function. This solver shows advantages when the model complexity is large.
- Multiple experimental results are provided to demonstrate the performance improvements in terms of classification accuracy and insensitivity to parameters achieved by the proposed method compared with state-of-the-art self-taught learning methods and other relevant techniques.

The rest of this paper is organized as follows. Section 2 introduces notations and overviews related work. The proposed framework and the corresponding optimization scheme are presented in Section 3. Experimental results and the corresponding analysis are provided in Section 4. Section 5 concludes with suggestions for future work.

2 BACKGROUND AND RELATED WORK

In this section, we introduce the paper’s notations and definitions and provide a review of techniques related to our proposed method.

In this paper, vectors are denoted by bold lowercase letters while matrices are denoted by bold uppercase letters. The superscript T of a matrix denotes the transposition operation. For a matrix \mathbf{A} , $\mathbf{A}^{(q)}$ denotes the q^{th} column and $\mathbf{A}_{(p)}$ denotes the p^{th} row, while $\mathbf{A}^{(p,q)}$ denotes the entry at the p^{th} row and q^{th} column. The $\ell_{r,p}$ -norm for a matrix $\mathbf{W} \in \mathbb{R}^{a \times b}$ is denoted as

$$\|\mathbf{W}\|_{r,p} = \left(\sum_{i=1}^a \left(\sum_{j=1}^b |\mathbf{W}^{(i,j)}|^r \right)^{p/r} \right)^{1/p}. \quad (1)$$

The trace of a matrix $\mathbf{L} \in \mathbb{R}^{a \times a}$ is defined as $\text{Tr}(\mathbf{L}) = \sum_{i=1}^a \mathbf{L}^{(i,i)}$. We use $\mathbf{1}$ and $\mathbf{0}$ to denote an all-ones and all-zeros matrix or vector of the appropriate size, respectively.

We use $\mathbf{X} = [\mathbf{X}^{(1)}, \mathbf{X}^{(2)}, \dots, \mathbf{X}^{(n)}] \in \mathbb{R}^{d \times n}$ to denote sample sets, where $\mathbf{X}^{(i)} \in \mathbb{R}^d$ is the i^{th} sample in \mathbf{X} for $i = 1, 2, \dots, n$, and where d and n denote data dimensionality and number of samples in \mathbf{X} , respectively.

For notations in transfer learning, we use \mathcal{D} to denote a domain and \mathcal{T} for a task. A domain \mathcal{D} consists of a feature space \mathcal{X} and a marginal probability distribution $P(\mathbf{X})$ over a sample set \mathbf{X} . A task \mathcal{T} consists of a label

space \mathcal{Y} and an objective predictive function $f(\mathbf{X}, \mathbf{Y})$ to predict the corresponding labels \mathbf{Y} of a sample set \mathbf{X} . We refer readers to [10] for a detailed explanation of these notations. In this paper we use $\mathcal{D}_{\text{src}} = \{\mathcal{X}_{\text{src}}, P(\mathbf{X}_{\text{src}})\}$ and $\mathcal{T}_{\text{src}} = \{\mathcal{Y}_{\text{src}}, f(\mathbf{X}_{\text{src}}, \mathbf{Y}_{\text{src}})\}$ to denote source domain and task, and use $\mathcal{D}_{\text{trg}} = \{\mathcal{X}_{\text{trg}}, P(\mathbf{X}_{\text{trg}})\}$ and $\mathcal{T}_{\text{trg}} = \{\mathcal{Y}_{\text{trg}}, f(\mathbf{X}_{\text{trg}}, \mathbf{Y}_{\text{trg}})\}$ for target domain and task.

2.1 Self-Taught Learning

Transfer learning methods can be classified as homogeneous and heterogeneous. Homogeneous transfer learning methods assume $\mathcal{X}_{\text{src}} = \mathcal{X}_{\text{trg}}$ while heterogeneous transfer learning methods assume $\mathcal{X}_{\text{src}} \neq \mathcal{X}_{\text{trg}}$. This paper focuses on homogeneous transfer learning.

Self-taught learning can be categorized into the group of inductive transfer learning methods [10], in which $\mathcal{T}_{\text{trg}} \neq \mathcal{T}_{\text{src}}$ while the domains can be either same or different. The idea of self-taught learning was first proposed by Raina et. al. [12] and implemented through dictionary learning and sparse coding.³ To be more specific, a dictionary is learned using source samples:

$$\begin{aligned} \min_{\mathbf{D}, \mathbf{A}_{\text{src}}} \|\mathbf{X}_{\text{src}} - \mathbf{D}\mathbf{A}_{\text{src}}\|_F^2 + \beta \sum_{i=1}^{n_{\text{src}}} \|\mathbf{A}_{\text{src}}^{(i)}\|_1, \\ \text{s.t. } \|\mathbf{D}^{(j)}\| \leq 1, 1 \leq j \leq s, \end{aligned} \quad (2)$$

where $\mathbf{D} \in \mathbb{R}^{d \times s}$ is a dictionary with each column as a dictionary element, and where each column in $\mathbf{A}_{\text{src}} \in \mathbb{R}^{s \times n_{\text{src}}}$ represents the sparse coefficient vector of the corresponding unlabeled source sample from $\mathbf{X}_{\text{src}} \in \mathbb{R}^{d \times n_{\text{src}}}$. After the dictionary \mathbf{D} is obtained, a new labeled training set $\{\mathbf{A}_{\text{trg}}, \mathbf{Y}_{\text{trg}}\}$ in the target domain is computed through

$$\min_{\mathbf{A}_{\text{trg}}} \|\mathbf{X}_{\text{trg}} - \mathbf{D}\mathbf{A}_{\text{trg}}\|_F^2 + \beta \sum_{i=1}^{n_{\text{trg}}} \|\mathbf{A}_{\text{trg}}^{(i)}\|_1, \quad (3)$$

where each column in $\mathbf{A}_{\text{trg}} \in \mathbb{R}^{s \times n_{\text{trg}}}$ represents the sparse coefficient vector of the corresponding labeled target sample from $\mathbf{X}_{\text{trg}} \in \mathbb{R}^{d \times n_{\text{trg}}}$. Finally, a classifier is learned on the new labeled training set by applying a supervised learning algorithm. The idea of self-taught learning has been applied in scenarios such as clustering [13], visual tracking [14], object localization [15, 16], hyperspectral image classification [17], wound infection detection [18], etc.

Wang et. al. [19] propose robust and discriminative self-taught learning (RDSTL) as an extension to STL. Compared with STL, two changes are made in order to increase the robustness of the learning model and make use of supervision information contained in target samples. The first is to replace the ℓ_1 -norm loss function used in STL with an $\ell_{2,1}$ -norm loss function because the latter is claimed to be more robust to noise and outliers. The second is to take advantage of label information of target samples during learning. Assume $\mathbf{X}_k \in \mathbb{R}^{d \times n_k}$ and $\mathbf{A}_k \in \mathbb{R}^{s \times n_k}$ denote the samples and corresponding sparse codes belonging to the k^{th} class. We refer to source samples as belonging to the 0^{th} class and assume that the dataset \mathbf{X} is arranged by

³ We use abbreviation STL to denote the method of [12] in the sequel, while we use the full name “self-taught learning” for the class of learning problems.

classes so that $\mathbf{X} = [\mathbf{X}_0, \mathbf{X}_1, \dots, \mathbf{X}_K]$, where K is the total number of classes in the target samples, with \mathbf{A} following the same setup. Then RDSTL can be written as the following optimization problem:

$$\begin{aligned} \min_{\mathbf{D}, \mathbf{A}} \|\mathbf{X} - \mathbf{D}\mathbf{A}\|_F^2 + \beta \sum_{k=0}^K \|\mathbf{A}_k^T\|_{2,1}, \\ \text{s.t. } \|\mathbf{D}^{(j)}\| \leq 1, 1 \leq j \leq s. \end{aligned} \quad (4)$$

Another advantage of imposing $\ell_{2,1}$ -norm regularization on the representation coefficients is that it makes the learning process insensitive to the dictionary size. This is because sparsity on rows of \mathbf{A} helps select basis vectors in \mathbf{D} : a basis vector contributes little to data representation if the ℓ_2 -norm value of its corresponding coefficient vector is close to 0. Therefore, the final task performance should not be sensitive to the dictionary size once it is large enough.

Li et. al. [20] proposes a self-taught low-rank (S-Low) coding framework which is suitable for both clustering and classification tasks in visual learning. By imposing a low-rank constraint onto the sparse coefficient matrix, S-Low coding is claimed to be able to characterize the global structure information in the target domain. The objective function of S-Low coding is

$$\begin{aligned} \min_{\mathbf{D}, \mathbf{A}_{\text{src}}, \mathbf{A}_{\text{trg}}, \mathbf{E}_{\text{src}}, \mathbf{E}_{\text{trg}}} \|\mathbf{A}_{\text{trg}}\|_{\gamma_1} + \lambda_1 M_{\gamma_2}(\mathbf{E}_{\text{src}}) + \\ \lambda_2 M_{\gamma_2}(\mathbf{E}_{\text{trg}}) + \lambda_3 \|\mathbf{A}_{\text{src}}\|_{2,1}, \\ \text{s.t. } \mathbf{X}_{\text{src}} = \mathbf{D}\mathbf{A}_{\text{src}} + \mathbf{E}_{\text{src}}, \mathbf{X}_{\text{trg}} = \mathbf{D}\mathbf{A}_{\text{trg}} + \mathbf{E}_{\text{trg}}, \end{aligned} \quad (5)$$

where $\|\cdot\|_{\gamma_1}$ denotes the matrix γ -norm with parameter γ_1 and $M_{\gamma_2}(\cdot)$ denotes the minimax concave penalty norm with parameter γ_2 . We refer readers to [20] for more details on the roles and definitions of these two norms.

Though the self-taught learning approaches mentioned above use different schemes for knowledge transfer, they all use the whole source sample set without considering their relevance to target domain, which makes these methods potentially vulnerable to negative transfer.

2.2 Single-Layer Autoencoder

A single-layer autoencoder is an artificial neural network that aims to reconstruct inputs by using only a single hidden layer. Given input data $\mathbf{x} \in \mathbb{R}^d$, an autoencoder first maps \mathbf{x} to a compressed data representation $\mathbf{z} \in \mathbb{R}^m$ in a hidden layer, given by $\mathbf{z} = f(\mathbf{W}_1\mathbf{x} + \mathbf{b}_1)$, where $\mathbf{W}_1 \in \mathbb{R}^{m \times d}$ is a weight matrix, $\mathbf{b}_1 \in \mathbb{R}^m$ is a bias vector, and $f(\cdot)$ is an elementary nonlinear activation function. This part is referred to as an *encoder*. Commonly used activation functions include the sigmoid function, the hyperbolic tangent function, the rectified linear unit, etc. The second step is to map the compressed data representation \mathbf{z} to output data $\bar{\mathbf{x}} \in \mathbb{R}^d$, which is $\bar{\mathbf{x}} = g(\mathbf{W}_2\mathbf{z} + \mathbf{b}_2)$, where $\mathbf{W}_2 \in \mathbb{R}^{d \times m}$ and $\mathbf{b}_2 \in \mathbb{R}^d$ are the corresponding weight matrix and bias vector, respectively. This part is referred to as a *decoder*.

The optimization problem underlying autoencoder training is to minimize the difference between the input data and the output data. To be more specific, given a set of data $\mathbf{X} = [\mathbf{X}^{(1)}, \mathbf{X}^{(2)}, \dots, \mathbf{X}^{(n)}]$, the parameters \mathbf{W}_1 , \mathbf{W}_2 , \mathbf{b}_1 , and \mathbf{b}_2 are adapted to minimize the reconstruction error $\sum_{i=1}^n \|\mathbf{X}^{(i)} - \bar{\mathbf{X}}^{(i)}\|_2^2$, where $\bar{\mathbf{X}}^{(i)}$ is the output of

autoencoder to the input $\mathbf{X}^{(i)}$. The general approach for this problem is the backpropagation algorithm [21].

3 PROPOSED METHOD

In this section, we introduce our proposed GASTL approach. The basic framework of GASTL is to reconstruct both source and target samples through a single-layer autoencoder, while simultaneously enforcing a linear relationship between source samples and target samples. Both global and local data structures are preserved through a single-layer autoencoder and spectral graph analysis, respectively. We develop a metric for the relevance between each source sample and target samples, which is used for source sample selection so that only samples with high relevance are selected for knowledge transfer. Meanwhile, a weight is assigned to each source sample reflecting its relevance to the target samples for the subsequent classifier training, during which each selected source sample is assigned a pseudo-label from the target domain label space and combined with target samples to build the classifier training sample set. Source sample weights are also considered during classifier training. Finally, the trained classifier is used to predict labels of unseen target samples.

3.1 Knowledge Transfer and Relevance Measure

In this section we present the problem formulation of our knowledge transfer scheme as well as the corresponding optimization. We also propose a measure for relevance between each source sample and target samples.

3.1.1 Objective Function

The objective function of GASTL includes four parts: a data reconstruction term, a domain mapping term, a regularization term for sample selection; and a term based on spectral graph analysis for local data structure preservation. The details of these four terms are described below.

Many transfer learning methods perform knowledge transfer from a source domain to a target domain by finding a mapping between them, that is, $h_1(\mathbf{X}_{\text{trg}}) = h_2(\mathbf{X}_{\text{src}})\mathbf{A}$, where $h_1(\cdot)$ and $h_2(\cdot)$ are two transformations, while \mathbf{A} is a matrix that linearly maps transformed source samples $h_2(\mathbf{X}_{\text{src}})$ into transformed target samples $h_1(\mathbf{X}_{\text{trg}})$. More specifically, the mapping is obtained from the optimization:

$$\min_{\Theta, \mathbf{A}} \mathcal{M}(\Theta, \mathbf{A}) + \lambda \mathcal{R}(\mathbf{A}), \quad (6)$$

where Θ is a set of parameters used for the nonlinear mappings h_1, h_2 , while $\mathcal{M}(\Theta, \mathbf{A}) = L(h_1(\mathbf{X}_{\text{trg}}), h_2(\mathbf{X}_{\text{src}})\mathbf{A})$ denotes a cost function for domain mapping, where $L(\cdot, \cdot)$ is a loss function and $\mathcal{R}(\cdot)$ corresponds to a regularization function on \mathbf{A} to avoid overfitting.⁴

A simple way to achieve domain mapping is to assume a linear mapping between source and target data, which is $\mathbf{X}_{\text{trg}} = \mathbf{X}_{\text{src}}\mathbf{A}$. This requires the cost $\mathcal{M}(\Theta, \mathbf{A}) = L(\mathbf{X}_{\text{trg}}, \mathbf{X}_{\text{src}}\mathbf{A})$. The use of a linear mapping in knowledge transfer is often computationally efficient. However, the success of this knowledge transfer scheme relies on an

4. We empirically found that regularizing Θ did not affect the performance of knowledge transfer much. Therefore, we do not pursue such regularization in this paper.

assumption that $\mathbf{X}_{\text{trg}} \in \text{span}(\mathbf{X}_{\text{src}})$ [22]. Due to the ubiquitous large discrepancy between source and target domain in self-taught learning scenarios, \mathbf{X}_{trg} is usually not in the span of \mathbf{X}_{src} , and hence a linear reconstruction scheme can hardly do well in knowledge transfer. Therefore, we need to find a non-linear reconstruction scheme that can decrease the discrepancy between source and target domains. One possible way to do this is to find a nonlinear transformation on \mathbf{X}_{trg} , and recover the output of this transformation as a linear transformation of source samples which are relevant to the target samples. That is, $\mathbf{h}(\mathbf{X}_{\text{trg}}) = \mathbf{X}_{\text{src}}\mathbf{A}$, where $\mathbf{h}(\cdot)$ is a nonlinear transformation. Furthermore, due to the possible large diversity of source samples compared with target samples, we can assume that the feature space shared by both source and target domains can be separated into several clusters: the source samples lie near a union of many clusters, while the target samples concentrate near a single cluster. Intuitively, negative transfer can be alleviated through using source samples close to target samples for knowledge transfer.

As mentioned in Section 2.2, a single-layer autoencoder aims at minimizing the reconstruction error between output and input data. We use $\mathbf{X} = [\mathbf{X}_{\text{src}} \ \mathbf{X}_{\text{trg}}]$ as the input to a single-layer autoencoder by optimizing a reconstruction error-driven loss function:

$$\mathcal{L}(\Theta) = \frac{1}{2n} \|\mathbf{X} - \mathbf{h}(\mathbf{X}; \Theta)\|_F^2, \quad (7)$$

where $n = n_{\text{src}} + n_{\text{trg}}$, $\Theta = [\mathbf{W}_1, \mathbf{W}_2, \mathbf{b}_1, \mathbf{b}_2]$, and $\mathbf{h}(\mathbf{X}; \Theta) = \mathbf{g}(\mathbf{W}_2 \cdot \mathbf{f}(\mathbf{W}_1\mathbf{X} + \mathbf{b}_1) + \mathbf{b}_2)$.⁵ We use the sigmoid function as the activation function: $\mathbf{f}(z) = \mathbf{g}(z) = 1/(1 + \exp(-z))$. In Eq. (7), both source and target samples share the same parameters to train an autoencoder, which makes the reconstructed source and target samples lie in the same submanifold under the learned parameters Θ . Meanwhile, we use the following minimization problem for the purpose of domain mapping:

$$\mathcal{C}(\Theta, \mathbf{A}) = \frac{1}{2n_{\text{trg}}} \|\mathbf{X}_{\text{src}}\mathbf{A} - \mathbf{h}(\mathbf{X}_{\text{trg}}; \Theta)\|_F^2. \quad (8)$$

That is, we enforce the target samples in the autoencoder output to be reconstructed by a linear combination of the source samples. While it is feasible to separate the optimization of Eq. (7) and Eq. (8), we observed that a joint framework is able to provide better knowledge transfer performance. Due to the nonlinear nature of transformation featured by a single-layer autoencoder, the distribution gap can be ameliorated through minimizing $\mathcal{C}(\Theta, \mathbf{A})$ with respect to Θ and \mathbf{A} . Therefore, we define the mapping cost

$$\mathcal{M}(\Theta, \mathbf{A}) = \mathcal{L}(\Theta) + \mu\mathcal{C}(\Theta, \mathbf{A}), \quad (9)$$

where μ is a balance parameter, to obtain a nonlinear mapping between source samples and target samples.

Since each row of \mathbf{A} indicates the importance of the corresponding source sample in reconstructing transformed target samples, we use the ℓ_2 -norm of each row of \mathbf{A} to measure the *relevance* between a source sample and target samples. This leads to an $\ell_{2,1}$ -norm regularization function

5. We often drop the dependence on Θ for readability, i.e. we use $\mathbf{h}(\mathbf{X})$ to denote $\mathbf{h}(\mathbf{X}; \Theta)$ when no ambiguity is caused.

$\mathcal{R}(\mathbf{A}) = \|\mathbf{A}\|_{2,1}$ that enforces row sparsity on the transformation matrix \mathbf{A} .

Data transformation based on autoencoders only guarantees broad data structure preservation, which does not take pair-wise relationship between data points into consideration. Therefore, we need to include local data geometric structures into our objective function. Local geometric structures of the data often contain discriminative information of neighboring data point pairs [23]. They assume that nearby data points should have similar representations. In order to characterize the local data structure, we construct a k -nearest neighbor (k NN) graph \mathbb{G} on the data space. The edge weight between two connected data points is determined by the similarity between those two points. We define the adjacency matrix \mathbf{S} for the graph \mathbb{G} as follows: for a data point $\mathbf{X}^{(i)}$, its weight $\mathbf{S}^{(i,j)} \neq 0$ if and only if $\mathbf{X}^{(i)} \in \mathcal{N}_k(\mathbf{X}^{(j)})$ or $\mathbf{X}^{(j)} \in \mathcal{N}_k(\mathbf{X}^{(i)})$, where $\mathcal{N}_k(\mathbf{X}^{(i)})$ denotes the k -nearest neighborhood set for $\mathbf{X}^{(i)}$; otherwise, $\mathbf{S}^{(i,j)} = 0$. In this paper, we use cosine distance to determine nonzero weight given by $\mathbf{S}^{(i,j)} = (\mathbf{X}^{(i)T}\mathbf{X}^{(j)})/(\|\mathbf{X}^{(i)}\|_2\|\mathbf{X}^{(j)}\|_2)$. The Laplacian matrix \mathbf{L} of the graph \mathbb{G} is defined as $\mathbf{L} = \mathbf{D} - \mathbf{S}$, where \mathbf{D} is a diagonal matrix whose i^{th} element on the diagonal is defined as $\mathbf{D}^{(i,i)} = \sum_{j=1}^n \mathbf{S}^{(i,j)}$. With these definitions, we set up the following minimization objective for local data structure preservation:

$$\begin{aligned} \mathcal{G}(\Theta) &= \frac{1}{2} \sum_{i=1}^n \sum_{j=1}^n \|\mathbf{z}^{(i)} - \mathbf{z}^{(j)}\|_2^2 \mathbf{S}^{(i,j)} \\ &= \sum_{i=1}^n \mathbf{z}^{(i)T} \mathbf{z}^{(i)} \mathbf{D}^{(i,i)} - \sum_{i=1}^n \sum_{j=1}^n \mathbf{z}^{(i)T} \mathbf{z}^{(j)} \mathbf{S}^{(i,j)} \quad (10) \\ &= \text{Tr}(\mathbf{Z}\mathbf{D}\mathbf{Z}^T) - \text{Tr}(\mathbf{Z}\mathbf{S}\mathbf{Z}^T) = \text{Tr}(\mathbf{Z}\mathbf{L}\mathbf{Z}^T), \end{aligned}$$

where $\mathbf{z}^{(i)} = \mathbf{f}(\mathbf{W}_1\mathbf{X}^{(i)} + \mathbf{b}_1)$ for $i = 1, 2, \dots, n$, and $\mathbf{Z} = [\mathbf{z}^{(1)}, \mathbf{z}^{(2)}, \dots, \mathbf{z}^{(n)}]$.

The final objective function of source sample selection can be written in terms of the following minimization with respect to the parameters $\Theta = [\mathbf{W}_1, \mathbf{W}_2, \mathbf{b}_1, \mathbf{b}_2]$ and \mathbf{A} :

$$\{\hat{\Theta}, \hat{\mathbf{A}}\} = \arg \min_{\Theta, \mathbf{A}} \mathcal{L}(\Theta) + \mu\mathcal{C}(\Theta, \mathbf{A}) + \lambda\mathcal{R}(\mathbf{A}) + \gamma\mathcal{G}(\Theta), \quad (11)$$

where μ , λ , and γ are balance parameters.

3.1.2 Optimization

The closed form solution of the optimization problem in Eq. (11) is hard to obtain due to the $\ell_{2,1}$ -norm regularization term. We employ an alternating optimization scheme to solve this problem with Θ and \mathbf{A} being iteratively updated, until the objective function value in Eq. (11) converges or a maximum number of iterations is reached.

When \mathbf{A} is fixed, Eq. (11) becomes

$$\hat{\Theta} = \arg \min_{\Theta} \mathcal{F}_1(\Theta) := \arg \min_{\Theta} \mathcal{L}(\Theta) + \mu\mathcal{C}(\Theta, \mathbf{A}) + \gamma\mathcal{G}(\Theta). \quad (12)$$

Following [24], we use a limited memory Broyden-Fletcher-Goldfarb-Shanno (L-BFGS) algorithm to solve Eq. (12). The L-BFGS algorithm has low computational cost, making it possible to use the whole dataset for optimization and provide more stable performance than commonly used stochastic gradient descent algorithms. For example, the dimensionality of the parameter Θ is the sum of the dimensionalities of $\mathbf{W}_1 \in \mathbb{R}^{m \times d}$, $\mathbf{W}_2 \in \mathbb{R}^{d \times m}$, $\mathbf{b}_1 \in \mathbb{R}^m$, and

$\mathbf{b}_2 \in \mathbb{R}^d$, which is $2md + d + m$. Compared with the conventional BFGS algorithm, which requires computing and storing of $(2md + d + m) \times (2md + d + m)$ Hessian matrices, the L-BFGS algorithm saves the past l updates of Θ and corresponding gradients. Therefore, denoting the number of iterations in the optimization by t , the corresponding computational complexity of L-BFGS is $O(tlmd)$. We refer readers to [25] for more details on L-BFGS algorithm, which we implement using the *minFunc* toolbox [26]. The solver requires the gradients of the objective function in Eq. (12) with respect to its parameters Θ . The gradients for both $\mathcal{L}(\Theta)$ and $\mathcal{C}(\Theta, \mathbf{A})$ can be obtained through a back-propagation algorithm. We skip the details for the derivation of the gradients of both $\mathcal{L}(\Theta)$ and $\mathcal{C}(\Theta)$, which are standard in the formulation of backpropagation for an autoencoder. The resulting gradients for $\mathcal{L}(\Theta)$ are:

$$\begin{aligned} \frac{\partial \mathcal{L}(\Theta)}{\partial \mathbf{W}_1} &= \frac{1}{n} \Delta_{\mathcal{L}_2} \mathbf{X}^T, & \frac{\partial \mathcal{L}(\Theta)}{\partial \mathbf{W}_2} &= \frac{1}{n} \Delta_{\mathcal{L}_3} \mathbf{Y}^T, \\ \frac{\partial \mathcal{L}(\Theta)}{\partial \mathbf{b}_1} &= \frac{1}{n} \Delta_{\mathcal{L}_2} \mathbf{1}, & \frac{\partial \mathcal{L}(\Theta)}{\partial \mathbf{b}_2} &= \frac{1}{n} \Delta_{\mathcal{L}_3} \mathbf{1}, \end{aligned} \quad (13)$$

where each column of $\Delta_{\mathcal{L}_2} \in \mathbb{R}^{m \times n}$ and $\Delta_{\mathcal{L}_3} \in \mathbb{R}^{d \times n}$ contains the error term of the corresponding sample for the hidden layer and the output layer, respectively:

$$\begin{aligned} \Delta_{\mathcal{L}_3} &= (\mathbf{h}(\mathbf{X}) - \mathbf{X}) \bullet \mathbf{h}(\mathbf{X}) \bullet (\mathbf{1} - \mathbf{h}(\mathbf{X})), \\ \Delta_{\mathcal{L}_2} &= (\mathbf{W}_2^T \Delta_{\mathcal{L}_3}) \bullet \mathbf{Y} \bullet (\mathbf{1} - \mathbf{Y}), \end{aligned}$$

with \bullet denoting the element-wise product operator. The gradients for $\mathcal{C}(\Theta, \mathbf{A})$ are:

$$\begin{aligned} \frac{\partial \mathcal{C}(\Theta, \mathbf{A})}{\partial \mathbf{W}_1} &= \frac{1}{n_{\text{trg}}} \Delta_{\mathcal{C}_2} (\mathbf{X}_{\text{src}} \mathbf{A})^T, & \frac{\partial \mathcal{C}(\Theta, \mathbf{A})}{\partial \mathbf{W}_2} &= \frac{1}{n_{\text{trg}}} \Delta_{\mathcal{C}_3} \mathbf{Y}_{\text{trg}}^T, \\ \frac{\partial \mathcal{C}(\Theta, \mathbf{A})}{\partial \mathbf{b}_1} &= \frac{1}{n_{\text{trg}}} \Delta_{\mathcal{C}_2} \mathbf{1}, & \frac{\partial \mathcal{C}(\Theta, \mathbf{A})}{\partial \mathbf{b}_2} &= \frac{1}{n_{\text{trg}}} \Delta_{\mathcal{C}_3} \mathbf{1}. \end{aligned} \quad (14)$$

Both $\Delta_{\mathcal{L}_2}^{(i)}$ and $\Delta_{\mathcal{L}_3}^{(i)}$ in Eq. (13) play same roles as $\Delta_{\mathcal{C}_2}^{(i)}$ and $\Delta_{\mathcal{C}_3}^{(i)}$ in Eq. (14). Their definitions are:

$$\begin{aligned} \Delta_{\mathcal{C}_3} &= (\mathbf{h}(\mathbf{X}_{\text{trg}}) - \mathbf{X}_{\text{src}} \mathbf{A}) \bullet \mathbf{h}(\mathbf{X}_{\text{trg}}) \bullet (\mathbf{1} - \mathbf{h}(\mathbf{X}_{\text{trg}})), \\ \Delta_{\mathcal{C}_2} &= (\mathbf{W}_2^T \Delta_{\mathcal{C}_3}) \bullet \mathbf{Y}_{\text{trg}} \bullet (\mathbf{1} - \mathbf{Y}_{\text{trg}}), \end{aligned}$$

where $\mathbf{Y}_{\text{trg}} = \mathbf{f}(\mathbf{W}_1 \mathbf{X}_{\text{trg}} + \mathbf{b}_1)$. The gradients of the graph term $\mathcal{G}(\Theta) = \text{Tr}(\mathbf{Y} \mathbf{L} \mathbf{Y}^T)$ can be obtained in a straightforward fashion as follows:

$$\begin{aligned} \frac{\partial \mathcal{G}(\Theta)}{\partial \mathbf{W}_1} &= \frac{\partial \text{Tr}(\mathbf{Y} \mathbf{L} \mathbf{Y}^T)}{\partial \mathbf{Y}} \cdot \frac{\partial \mathbf{Y}}{\partial \mathbf{W}_1} = 2(\mathbf{Y} \mathbf{L} \bullet \mathbf{Y} \bullet (\mathbf{1} - \mathbf{Y})) \mathbf{X}^T, \\ \frac{\partial \mathcal{G}(\Theta)}{\partial \mathbf{W}_2} &= \mathbf{0}, \\ \frac{\partial \mathcal{G}(\Theta)}{\partial \mathbf{b}_1} &= \frac{\partial \text{Tr}(\mathbf{Y} \mathbf{L} \mathbf{Y}^T)}{\partial \mathbf{Y}} \cdot \frac{\partial \mathbf{Y}}{\partial \mathbf{b}_1} = 2(\mathbf{Y} \mathbf{L} \bullet \mathbf{Y} \bullet (\mathbf{1} - \mathbf{Y})) \mathbf{1}, \\ \frac{\partial \mathcal{G}(\Theta)}{\partial \mathbf{b}_2} &= \mathbf{0}. \end{aligned}$$

To conclude, the gradients of the objective function in Eq. (12) with respect to $\Theta = [\mathbf{W}_1, \mathbf{W}_2, \mathbf{b}_1, \mathbf{b}_2]$ can be written as

$$\begin{aligned} \frac{\partial \mathcal{F}_1(\Theta)}{\partial \mathbf{W}_1} &= \frac{1}{n} \Delta_{\mathcal{L}_2} \mathbf{X}^T + \frac{\mu}{n_{\text{trg}}} \Delta_{\mathcal{C}_2} (\mathbf{X}_{\text{src}} \mathbf{A})^T \\ &\quad + 2\gamma (\mathbf{Y} \mathbf{L} \bullet \mathbf{Y} \bullet (\mathbf{1} - \mathbf{Y})) \mathbf{X}^T, \\ \frac{\partial \mathcal{F}_1(\Theta)}{\partial \mathbf{W}_2} &= \frac{1}{n} \Delta_{\mathcal{L}_3} \mathbf{Y}^T + \frac{\mu}{n_{\text{trg}}} \Delta_{\mathcal{C}_3} \mathbf{Y}_{\text{trg}}^T, \\ \frac{\partial \mathcal{F}_1(\Theta)}{\partial \mathbf{b}_1} &= \frac{1}{n} \Delta_{\mathcal{L}_2} \mathbf{1} + \frac{\mu}{n_{\text{trg}}} \Delta_{\mathcal{C}_2} \mathbf{1} + 2\gamma (\mathbf{Y} \mathbf{L} \bullet \mathbf{Y} \bullet (\mathbf{1} - \mathbf{Y})) \mathbf{1}, \\ \frac{\partial \mathcal{F}_1(\Theta)}{\partial \mathbf{b}_2} &= \frac{1}{n} \Delta_{\mathcal{L}_3} \mathbf{1} + \frac{\mu}{n_{\text{trg}}} \Delta_{\mathcal{C}_3} \mathbf{1}. \end{aligned}$$

When Θ is fixed, Eq. (11) becomes

$$\hat{\mathbf{A}} = \arg \min_{\mathbf{A}} \mathcal{F}_2(\mathbf{A}) := \arg \min_{\mathbf{A}} \mu \mathcal{C}(\Theta, \mathbf{A}) + \lambda \mathcal{R}(\mathbf{A}). \quad (15)$$

Following [27], we use the scheme described below to optimize \mathbf{A} . The regularization term $\mathcal{R}(\mathbf{A}) = \|\mathbf{A}\|_{2,1}$ and its derivative do not exist for its i^{th} column $\mathbf{A}^{(i)}$ when $\mathbf{A}^{(i)} = \mathbf{0}$. In this case, we calculate the values of elements in $\mathbf{A} \mathbf{U}$ to approximate the derivative of $\mathcal{R}(\mathbf{A})$ with respect to \mathbf{A} , where $\mathbf{U} \in \mathbb{R}^{d \times d}$ is a diagonal matrix whose i^{th} element on the diagonal is

$$\mathbf{U}^{(i,i)} = \begin{cases} \left(\|\mathbf{A}^{(i)}\|_2 + \epsilon \right)^{-1}, & \|\mathbf{A}^{(i)}\|_2 \neq 0, \\ 0, & \text{otherwise,} \end{cases} \quad (16)$$

where ϵ is a small constant added to avoid overflow. Since $\mathcal{R}(\mathbf{A}) = \|\mathbf{A}\|_{2,1}$ is not differentiable when the ℓ_2 -norm of a certain row in \mathbf{A} is 0, we calculate the subgradient for each element in \mathbf{A} for that case. That is, for each element in \mathbf{A} , the subgradient at 0 can be an arbitrary value in the interval $[-1, 1]$, and so we set the gradient to 0 for computational convenience. In this way, the subgradient of $\mathcal{F}_2(\mathbf{A})$ with respect to \mathbf{A} is:

$$\frac{\partial \mathcal{F}_2(\mathbf{A})}{\partial \mathbf{A}} = \frac{\mu}{n_{\text{trg}}} [\mathbf{X}_{\text{src}}^T \mathbf{X}_{\text{src}} \mathbf{A} - \mathbf{X}_{\text{src}}^T \mathbf{h}(\mathbf{X}_{\text{trg}})] + \lambda \mathbf{A} \mathbf{U}. \quad (17)$$

That is, when \mathbf{U} is fixed, an optimal value of \mathbf{A} can be obtained through

$$\hat{\mathbf{A}} = (\mu \mathbf{X}_{\text{src}}^T \mathbf{X}_{\text{src}} + n_{\text{trg}} \lambda \mathbf{U})^{-1} \mu \mathbf{X}_{\text{src}}^T \mathbf{h}(\mathbf{X}_{\text{trg}}). \quad (18)$$

Therefore, we can update \mathbf{U} through Eq. (16) when \mathbf{A} is fixed and update \mathbf{A} through Eq. (18) when \mathbf{U} is fixed with an iterative scheme until the value of $\mathcal{F}_2(\mathbf{A})$ converges.

3.2 Classifier Training

The next step is to use source samples combined with target samples to train a classifier, which can then be applied to unseen samples in the target domain for classification. Since source samples have different relevance levels with the target domain, we propose a scheme to assign weights to source samples that reflect their relevance. Source domain samples with large weights are kept while others are discarded. Subsequently, a classifier is trained using both target samples and selected source samples. For each source sample, pseudo-labels that indicate the transferability of the source sample to different target classes are used as true labels during classifier training, where transferability [28] reflects the possibility of transferring a source sample to a target domain class. The transferability values of source samples are stored in a matrix $\mathbf{Tr} \in \mathbb{R}^{n_{\text{src}} \times n_{\text{ctrg}}}$, where n_{ctrg} is the cardinality of \mathcal{Y}_{trg} . Two pseudo-labeling schemes are proposed for comparison. Additionally, source sample weights are taken into consideration in classifier training. For each pseudo-labeling scheme, we evaluate both soft and hard classification with the softmax classifier.

3.2.1 Source Domain Sample Reweighting

As mentioned in Section 3.1.1, the ℓ_2 -norm value of each row of \mathbf{A} can be used to measure the relevance between the corresponding source sample and target samples. We propose a scheme to assign a weight to each source sample based on

the corresponding row in \mathbf{A} . The weight for a source sample $\mathbf{X}_{\text{src}}^{(i)}|_{i=1}^{n_{\text{src}}}$ is set as the ℓ_2 -norm value of the corresponding row in \mathbf{A} . That is, for a source sample $\mathbf{X}_{\text{src}}^{(i)}$, its weight vector $\mathbf{Wt} \in \mathbb{R}^{n_{\text{src}}}$ has entries $\mathbf{Wt}(i) = \|\mathbf{A}_{(i)}\|_2 / \max_j (\|\mathbf{A}_{(j)}\|_2)$. Note that the vector \mathbf{Wt} is normalized with the maximum entry value being 1. In addition, during classifier training, all target training samples are given weight 1.

3.2.2 Pseudo-Labeling

Two transferability measure schemes are proposed and pseudo-labels are assigned to source samples based on transferability values.

Scheme A: For a given source sample $\mathbf{X}_{\text{src}}^{(i)}$, its transferability to a target class $\mathbf{c}^{(j)}$ is measured by the square of the ℓ_2 -norm of a subvector consisting of elements in the corresponding row of \mathbf{A} that belong to target samples of $\mathbf{c}^{(j)}$. That is, $\mathbf{Tr}^{(i, \mathbf{c}^{(j)})} = \|\mathbf{A}^{(i, \mathbf{J}_{\mathbf{c}^{(j)}})}\|_2^2$, where $\mathbf{J}_{\mathbf{c}^{(j)}}$ denotes the columns in \mathbf{A} that correspond to class $\mathbf{c}^{(j)}$.

Scheme B: By following [28], we adopt the isometric Gaussian probability [29] computed on the hidden layer representation of the trained single-layer autoencoder as the transferability of a given source sample $\mathbf{X}_{\text{src}}^{(i)}$ to a target class $\mathbf{c}^{(j)}$. More concretely, the transferability is

$$\mathbf{Tr}^{(i, \mathbf{c}^{(j)})} = \mathcal{N}(\mathbf{Z}_{\text{src}}^{(i)} | \bar{\mathbf{Z}}_{\text{trg}}^{\mathbf{c}^{(j)}}, \sigma^2 \mathbf{I}), \quad (19)$$

where $\mathbf{Z}_{\text{src}}^{(i)} \in \mathbb{R}^m$ is the hidden layer representation of the source sample $\mathbf{X}_{\text{src}}^{(i)}$, and $\bar{\mathbf{Z}}_{\text{trg}}^{\mathbf{c}^{(j)}} \in \mathbb{R}^m$ is the mean of the hidden layer representation of target samples belonging to class $\mathbf{c}^{(j)}$. As such, the transferability is measured by the probability that the source sample belongs to a target class given the auxiliary information $\bar{\mathbf{Z}}_{\text{trg}}^{\mathbf{c}^{(j)}}$.

The pseudo-labels of source samples consist of a matrix $\mathbf{L} \in \mathbb{R}^{n_{\text{src}} \times n_{\text{ctr}}}$. We assign pseudo-labels to source samples based on their transferability values to different target domain classes. Given a source sample $\mathbf{X}_{\text{src}}^{(i)}$, for a **hard classifier**, we set $\mathbf{L}^{(i, j)} = 1$ if target class $\mathbf{c}^{(j)}$ provides the largest transferability value; otherwise $\mathbf{L}^{(i, j)} = 0$. For a **soft classifier**, the normalized transferability values are used as pseudo-labels so that pseudo labels reflect the likelihood of transferring source samples to target domain classes: $\mathbf{L}^{(i, j)} = \mathbf{Tr}^{(i, \mathbf{c}^{(j)})} / \sum_{k=1}^{n_{\text{ctr}}} \mathbf{Tr}^{(i, \mathbf{c}^{(k)})}$. Compared with hard classifiers, soft classifiers may help improve knowledge transfer performance since it is able to capture the relationship between each single source sample and multiple target categories instead of one. This is especially necessary for image classification tasks since there usually exists commonalities between image categories.

3.2.3 Classifier Training

We employ softmax classifier due to its simplicity and capability to do soft classification. The training data weights are included in classifier training, which leads to the following cost function

$$J(\Theta_{\mathbf{c}}) = -\frac{1}{n} \left[\sum_{i=1}^n \mathbf{Wt}(i) \sum_{j=1}^{n_{\text{ctr}}} \mathbf{L}^{(i, j)} \log \frac{e^{\Theta_{\mathbf{c}}^{(j)T} \mathbf{X}^{(i)}}}{\sum_{l=1}^{n_{\text{ctr}}} e^{\Theta_{\mathbf{c}}^{(l)T} \mathbf{X}^{(i)}}} \right],$$

where $\Theta_{\mathbf{c}} = [\Theta_{\mathbf{c}}^{(1)}, \Theta_{\mathbf{c}}^{(2)}, \dots, \Theta_{\mathbf{c}}^{(n_{\text{ctr}})}]$ is the classifier parameter to be optimized. We use an L-BFGS algorithm to

compute the optimal value of Θ . The gradients needed for optimization are given by

$$\frac{\partial J(\Theta_{\mathbf{c}})}{\partial \Theta_{\mathbf{c}}^{(j)}} = -\frac{1}{n} \sum_{i=1}^n \left[\mathbf{Wt}(i) \mathbf{X}^{(i)} \left(\mathbf{L}^{(i, j)} - \frac{e^{\Theta_{\mathbf{c}}^{(j)T} \mathbf{X}^{(i)}}}{\sum_{l=1}^{n_{\text{ctr}}} e^{\Theta_{\mathbf{c}}^{(l)T} \mathbf{X}^{(i)}}} \right) \right].$$

4 EXPERIMENTS

In this section, we evaluate the knowledge transfer performance of GASTL. Experiments are conducted on four benchmark datasets covering computer vision, natural language processing, and speech recognition. We also compare GASTL with other relevant state-of-the-art transfer learning techniques. To be more specific, we first select p source samples which are the most relevant to the target domain, and then use those selected source samples combined with labeled target samples to train a classifier. The classification rates on target testing samples are then used as metric to evaluate knowledge transfer performance.

4.1 Dataset Preparation

We introduce the information of datasets we use in our experiments. We first provide the overall information of each dataset. After that we introduce the source/target domain setup.

- **Dataset Information:** We employ four benchmark datasets in our experiments, including one visual dataset (Caltech101⁶), two natural language datasets (IMDB⁷ and Twitter,⁸ both for sentiment analysis), and one audio dataset (ESC-50⁹). In order to eliminate the side effects caused by imbalanced classes, we set the number of samples from each class to be the same within each dataset through random selection. For Caltech101, we keep 30 images for each class. For both IMDB and Twitter, we only consider texts with no more than 10 words. The ESC-50 dataset already has an even class setup with each class containing 40 audio clips. The properties of these datasets are summarized in Table 1.
- **Feature Extraction:** Data in raw feature space cannot be used for knowledge transfer due to possible dimensionality inconsistency. For example, images may have different sizes and texts may have different lengths. Therefore, it is necessary to do feature extraction on each dataset to make knowledge transfer feasible. For Caltech101, we employ two types of features. The first one is the 1,000-dimensional SIFT-BOW feature¹⁰ proposed in Gehler et al. [30]. The second one is the 4,096-dimensional output of

6. Dataset downloaded from: http://www.vision.caltech.edu/Image_Datasets/Caltech101/. The Caltech101 dataset contains both a "Faces" and "Faces easy" class, with each consisting of different versions of the same human face images. However, the images in "Faces" contain more complex backgrounds. To avoid confusion between these two similar classes of images, we do not include the "Faces easy" images in our experiments. Therefore, we keep 100 classes for Caltech101.

7. Dataset downloaded from: <https://drive.google.com/file/d/0B8yp1gOBCztyN0JaMDVoeXhHWm8/>.

8. Dataset downloaded from: <https://www.kaggle.com/c/twitter-sentiment-analysis2/data>

9. Dataset downloaded from: <https://github.com/karoldvl/ESC-50>

10. Dataset downloaded from: <http://files.is.tue.mpg.de/pgehler/projects/iccv09/>.

TABLE 1
Details of datasets used in our experiment.

Dataset	Features	Samples	Classes	Type
Caltech101 (SIFT-BOW)	1,000	3,000	100	Image
Caltech101 (VGG-19)	4,096	3,000	100	Image
IMDB	3,000	6,500	2	Text
Twitter	3,000	6,500	2	Text
ESC-50	2,592	2,000	50	Audio

the last fully connected layer of the pre-trained VGG-19 model [31]. In our experiments we use the Keras tool¹¹ to compute the VGG-19 features.¹² For both IMDB and Twitter, we use the method from [32]¹³ to do feature extraction. By using a convolutional neural network model with publicly available WORD2VEC vectors, we get a 300×10 matrix for each text, which forms a 3,000-dimensional feature vector after column concatenation. We denote this feature as WORD2VEC in the sequel. For ESC-50, by following [33], we use the librosa package [34] to compute mel-frequency cepstral coefficients (MFCC) for each clip. After discarding the 0th coefficient, the first 12 MFCCs are whitened and used as feature for each clip. Therefore, we get a 12×216 matrix for each clip,¹⁴ which forms a 2,592-dimensional vector after column concatenation. These 2,592-dimensional vectors are used as features for audio clips. We denote this feature as MFCC in the sequel.

- **Source/Target Split:** For Caltech101, we randomly separate the 100 classes into 5 groups with 20 classes in each group. Five independent self-taught learning experiments were conducted on Caltech101: in each experiment samples in one group are used as target samples and those in the remaining four groups are used as source samples. For each class in the target domain, 15 samples were used for training and 15 samples were used for testing. For the two natural language datasets, we used one as source and the other one as target. That is, when IMDB was used as target, then Twitter was used as source and vice versa. For computational convenience, we did not use the entire datasets when either IMDB and Twitter is used as the source. We randomly selected 3,000 samples as source for both IMDB and Twitter. For each class in the target domain, 10, 100, 1000 samples were used for training and 750 samples were used for testing. The audio clips in ESC-50 dataset are separated into 5 groups with each group containing 10 classes. The 5 groups are: animal sounds; natural soundscapes and water sounds; human, non-speech sounds; interior/domestic sounds; and exterior/urban noises. Like Caltech101, we conducted five independent self-taught learning experiments on ESC-50 that in each experiment samples in one category were used as target and those in the other four categories were used as source. For each class in the target domain of ESC-50, 5, 10, 15, 20 samples were used for training and 20 samples were used for testing.

11. We refer readers to <https://github.com/keras-team/keras> for more information on Keras.

12. In the sequel, we use VGG-19 to denote the feature generated by VGG-19 models.

13. Codes downloaded from: https://github.com/yoonkim/CNN_sentence

14. Each MFCC contains 216 frames in our experiments.

4.2 Experimental Setup

We performed classification on the target testing samples in order to evaluate the effectiveness of the self-taught learning algorithms and two sample selection/re-weighting based domain adaptation methods. The three self-taught learning methods are STL [12], RDSTL [19], and S-Low [20] introduced in Section 2.1. The two domain adaptation methods are kernel mean matching (KMM) [35] and multiscale landmarks selection (MLS) [36]. These two domain adaptation methods were tailored to the scenario of self-taught learning. We also compute the classification performance without knowledge transfer.

Both GASTL and the compared algorithms include parameters to adjust. In this experiment, we fix some parameters and tune others through a grid search strategy. For algorithms requiring source sample selection/re-weighting, we select the number of source samples $p \in \{10, 20, 30, \dots, 100, 150, 200, 250, \dots, 500, 1000, 1500, n_{src}\}$. In GASTL, the range of hidden layer sizes is set to $m \in \{10, 50, 100, 200\}$, while the balance parameters are given ranges of $\lambda \in \{10^{-4}, 10^{-3}, 10^{-2}, 10^{-1}, 1\}$ and $\gamma \in \{0, 10^{-4}, 10^{-3}, 10^{-2}, 10^{-1}\}$. The value of μ is set to 1. The number of nearest neighbor in a k NN graph is set to 5. The value of σ^2 is set to 1.

All three self-taught learning methods (STL, RDSTL, and S-Low) are based on dictionary learning, and sparse code vectors were used as features for classification. For STL, we first performed PCA on each training sample since the features listed in Table 1 have high dimensionalities and require large dictionary sizes, which would cause prohibitive training time. Following [12], we kept the number of principal components to preserve approximately 96% of the training sample variance. We also found empirically that small dictionary sizes provide poor performance and large dictionary sizes result in unfeasibly long training times. In this experiment, we empirically set the dictionary size as the training set size, which are 2,400 for Caltech101, 3,000 for both IMDB and Twitter, and 1,600 for ESC-50, for their acceptable training time and good performance.

The balance parameter β in Eq. (2) and Eq. (3) is sampled from $\beta \in \{10^{-6}, 10^{-5}, 10^{-4}, 10^{-3}, 10^{-2}, 10^{-1}\}$. For both RDSTL and S-Low, we observed that their performance was not very sensitive to dictionary sizes but quite dependent on balance parameters. Therefore, we use the following parameter adjustment scheme. For RDSTL, we first use grid search for parameter β with the range $\{10^{-9}, 10^{-8}, \dots, 10^{-1}, 1\}$. The parameter value leading to the highest classification accuracy, denoted by $\hat{\beta}_1$, is kept for the next round. Assume $\hat{\beta}_1 = a_1 \times 10^{b_1}$, then the second round of grid search is of the range $\{a_1 - 0.4, \dots, a_1 - 0.1, a_1 + 0.1, \dots, a_1 + 0.5\} \times 10^{b_1}$. The parameter value that resulted in the best classification performance in the second round is denoted as $\hat{\beta}_2$. Assume $\hat{\beta}_2 = a_2 \times 10^{b_2}$, then the third round of grid search is of the range $\{a_2 - 0.04, \dots, a_2 - 0.01, a_2 + 0.01, \dots, a_2 + 0.05\} \times 10^{b_2}$. The parameter value that resulted in the best classification performance in the third round is denoted as $\hat{\beta}_3$, which is the final optimal β value. For S-Low, both λ_1 and λ_2 are set to 0.02 and we also use a three-round scheme to adjust the value of λ_3 . The initial range of λ_3 is $\{10^{-5}, 10^{-4}, \dots, 10^{-1}, 1\}$. Due to the large time consump-

tion during parameter adjusting, we also perform PCA with the same scheme that are used for STL.

For both KMM¹⁵ and MLS¹⁶, we first obtained weights for the source samples, which are also assigned pseudo-labels. Between the two pseudo-labeling schemes described in Section 3.2, only Scheme B is applicable since Scheme A is dependent on the transformation matrix \mathbf{A} , and these two domain adaptation methods do not generate one. We use the features listed in Table 1 in Eq. (19) instead of autoencoder activations as we did in GASTL. Subsequent steps were exactly the same as those for GASTL. For the optimization of GASTL with L-BFGS, we set the number of iterations t to be 400 and the number of storing updates l to be 100.

4.3 Parameter Sensitivity

We study the performance variation of GASTL with respect to the hidden layer size m and the two balance parameters λ and γ reflected by classification accuracy on target testing samples. We show the results on all four datasets.

We first study the parameter sensitivity of GASTL with respect to the hidden layer size m . Due to limited space, we only present a small portion of our experimental results in Fig. 1,¹⁷ where ‘‘Soft’’ and ‘‘Hard’’ refer to whether a soft or hard classifier is used, while ‘‘A’’ and ‘‘B’’ refer to the pseudo-labeling schemes. Note that although we train classifiers with multiple choices of source sample numbers, the classification results in Fig. 1 are the highest classification accuracy among all available choices. The results show that the performance of GASTL is not too sensitive to hidden layer size on the given datasets.

We also study the parameter sensitivity of GASTL with respect to the balance parameters λ and γ , under a fixed hidden layer size. In order to do this, with all other parameters being fixed, we record the classification accuracy corresponding to each parameter combination, which consists of a 5×5 matrix. We then calculate the mean and standard deviation of these 25 elements, and parameter sensitivity can be evaluated through the ratio between standard deviation and mean value. We choose hidden layer size $m = 10$ as Fig. 1 shows that the performance of GASTL is not sensitive to the value of m . The results are listed in Table 2, where we can find that the performance of GASTL is quite stable with respect to the balance parameters λ and γ for Caltech101, IMDB, and Twitter. For ESC-50, the standard deviation values are relatively large compared with the mean values.

4.4 Performance Comparison

We present the classification accuracy results of GASTL and baselines on all datasets in Tables 3 to 7, corresponding to Caltech101 (SIFT-BOW), Caltech101 (VGG-19), IMDB, Twitter, and ESC-50¹⁸, respectively. Note that ‘‘Target Only’’

15. Codes downloaded from: <http://www.gatsby.ucl.ac.uk/~gretton/covariateShiftFiles/covariateShiftSoftware.html>

16. Codes downloaded from: <https://github.com/jindongwang/transferlearning/tree/master/code>

17. For Caltech101, we use the results of one set out of five with SIFTBOW features as autoencoder inputs. For both IMDB and Twitter, we use the results with each target data having 10 training samples. For ESC-50, we use the results of one set out of five with each target data having 10 training samples.

18. Due to limited space, for ESC-50 we only perform results with 10 training samples for each target class.

TABLE 2
Performance stability of GASTL in classification with respect to balance parameters λ and γ . Classification accuracy mean (%) and standard deviation (%) are presented.

Dataset Scheme	Caltech101 (SIFT- BOW)	Caltech101 (VGG-19)	IMDB	Twitter	ESC-50
SoftA	48.92 \pm 1.53	94.48 \pm 0.47	58.22 \pm 0.60	55.79 \pm 0.47	21.54 \pm 1.38
HardA	44.20 \pm 1.17	92.84 \pm 1.45	57.91 \pm 0.98	55.41 \pm 1.13	20.06 \pm 2.15
SoftB	48.75 \pm 1.65	94.44 \pm 0.51	58.08 \pm 0.54	55.76 \pm 0.47	21.68 \pm 1.46
HardB	44.27 \pm 1.45	94.39 \pm 1.20	57.79 \pm 0.86	55.06 \pm 1.29	20.58 \pm 2.11

TABLE 3
Performance of GASTL and competing feature selection algorithms in classification on Caltech101 with SIFTBOW as feature. Classification accuracy (%) is used as the evaluation metric.

Set ID Method	1	2	3	4	5
Target Only	42.33	61.67	42.33	48.33	46.00
STL	46.00	64.33	48.33	46.33	56.00
RDSTL	36.67	51.33	37.00	39.67	42.00
S-Low	35.00	51.00	36.67	34.33	36.67
KMM-Soft	48.67	66.00	47.33	52.67	56.33
KMM-Hard	43.67	63.67	43.33	47.67	48.33
MLS-Soft	47.33	66.33	47.67	51.67	53.33
MLS-Hard	45.33	62.00	42.00	46.00	47.67
GASTL-SoftA	53.00	67.67	51.67	56.00	58.67
GASTL-HardA	47.67	64.33	47.67	48.67	52.33
GASTL-SoftB	52.33	68.00	51.33	53.33	58.67
GASTL-HardB	48.00	64.00	46.33	49.33	51.00

denotes the method that performs classification on target samples without knowledge transfer. In Tables 3, 4, and 7 each column corresponds to one subset, while in Tables 5 and 6, each column corresponds to one training sample number in each target class. We highlight the best two performances in each experiment given that we find in many cases the best two (or even more) performance are very close to each other.

We first provide an overall description on the comparison between GASTL and the competitors on each dataset. We can find that in Tables 3 and 4 the best performances are claimed by GASTL methods. In Tables 5 and 6, RDSTL is comparable to GASTL in a few cases, while in Table 7, the advantages of GASTL over RDSTL are sometimes small. In other words, GASTL provides the best overall performance. We can also find that the classification performance of the two pseudo-labeling schemes are quite similar to each other in almost every case in the five tables. Our next analysis focuses on the comparison between performance generated by soft classifiers and hard classifiers.

In Table 3, it is obvious that GASTL methods with soft classifiers provide the best performance. For image datasets such as Caltech101, it is unusual for the relevance between one source sample and a particular target class to be much larger than for other target classes. A soft classifier is able to characterize the relationship between a source sample and each target class during pseudo-labeling, while a hard classifier only selects the most similar class to each source sample and ignores other target classes, which may degrade knowledge transfer performance due to the possible useful

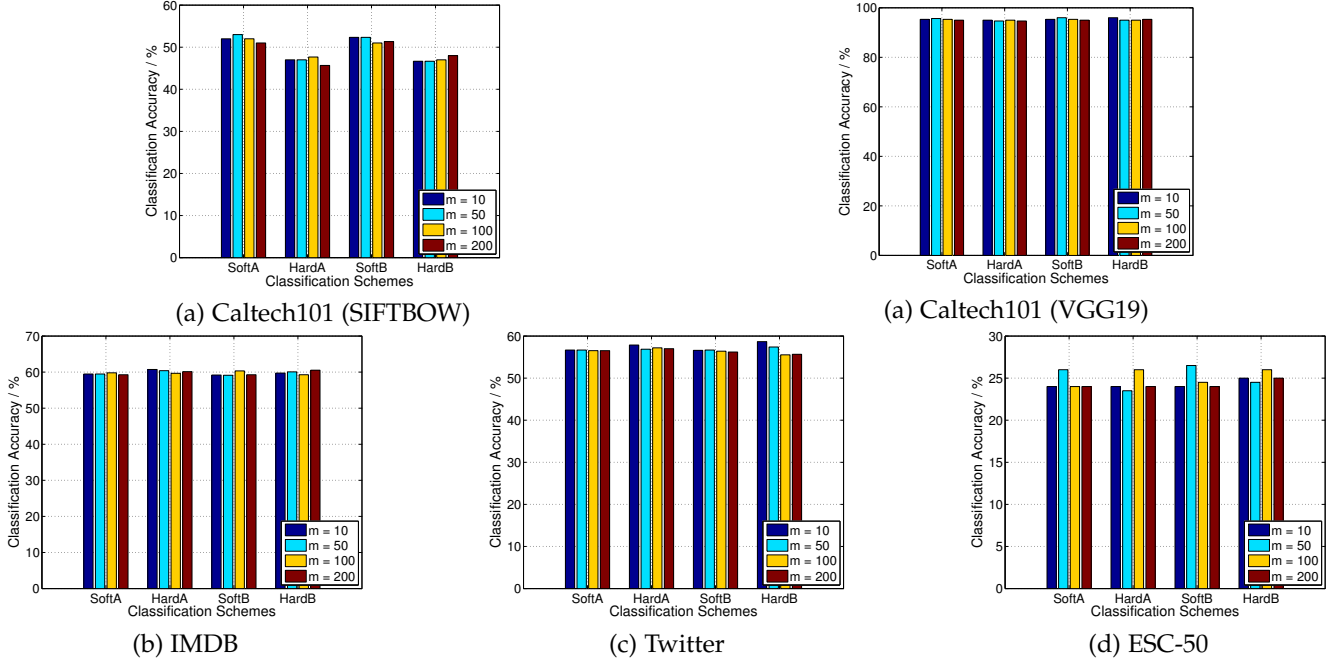


Fig. 1. Performance of GASTL in classification as a function of the hidden layer size m for varying sizes of the autoencoder hidden layer m . Classification accuracy (%) is used as the evaluation metric.

TABLE 4

Performance of GASTL and competing feature selection algorithms in classification on Caltech101 with VGG19 as feature. Classification accuracy (%) is used as the evaluation metric.

Set ID \ Method	1	2	3	4	5
Target Only	94.33	95.67	93.00	94.33	93.67
STL	95.00	95.33	92.00	94.67	94.33
RDSTL	91.67	93.00	85.67	90.00	89.33
S-Low	91.33	90.67	87.00	89.67	89.33
KMM-Soft	95.33	96.00	93.33	93.67	94.67
KMM-Hard	94.33	95.33	92.33	94.00	93.67
MLS-Soft	94.00	95.33	92.67	94.00	93.67
MLS-Hard	95.00	95.67	93.00	94.33	93.67
GASTL-SoftA	95.67	97.00	93.67	95.00	96.00
GASTL-HardA	95.00	97.00	94.67	95.67	96.00
GASTL-SoftB	96.00	97.00	93.67	94.67	96.00
GASTL-HardB	96.00	96.67	94.67	95.67	95.67

information from other classes. This can also be validated by the results of KMM and MLS in Table 3, which shows the advantages of soft classifiers over hard classifiers. However, the classification rates listed in Table 4 are quite large and similar to each other. Therefore, these results cannot provide significant information on validating the advantages of soft classifier over hard classifier on image datasets. On the other hand, the performance increase brought by knowledge transfer also depends on the difficulty of the classification problem. For example, the performance increase of Caltech101 using the SIFT-BOW features is much larger than using the VGG-19 features.

In Tables 5 and 6, hard classifiers consistently provide slightly better performance than soft classifiers for GASTL methods, while for KMM and MLS, the differences are smaller. According to our experimental setup, IMDB and Twitter play interchangeable roles as source and target. Therefore, in each experiment both source and target do-

TABLE 5

Performance of GASTL and competing feature selection algorithms in classification on IMDB. Classification accuracy (%) is used as the evaluation metric. TS = Training sample number in each target class.

Method \ TS	10	100	1000
Target Only	57.60	68.20	73.27
STL	58.80	69.53	73.73
RDSTL	60.53	70.47	73.47
S-Low	59.93	64.87	73.07
KMM-Soft	57.13	69.13	73.53
KMM-Hard	58.00	68.60	73.33
MLS-Soft	56.40	68.47	72.87
MLS-Hard	56.80	68.80	72.53
GASTL-SoftA	59.80	69.33	74.60
GASTL-HardA	60.73	70.47	77.67
GASTL-SoftB	60.33	69.27	74.47
GASTL-HardB	60.53	70.60	77.67

mains share a label space with two labels (“positive sentiment” and “negative sentiment”). Therefore, in this case it is better to use hard classifier than soft classifier since the two labels indicate two mutually exclusive categories.

It is difficult to interpret the results in Table 7. The overall performance of hard classifier based methods is better than soft classifier based ones for groups 1 to 4, while group 5 provides opposite results. We believe that the results reflect the complexity of this dataset.

4.5 Discussion

4.5.1 The Effect of Local Data Structure Preservation

As mentioned in Section 3.1.1, local data structure preservation provides similar representation for nearby data points. Intuitively, local data structure preservation applied in the hidden layer of the autoencoder is likely to improve knowledge transfer performance because it is able to reduce hidden layer representation distortion as they are involved

TABLE 6

Performance of GASTL and competing feature selection algorithms in classification on Twitter. Classification accuracy (%) is used as the evaluation metric. TS = Training sample number in each target class.

Method \ TS	10	100	1000
Target Only	55.47	58.93	77.80
STL	53.67	58.93	76.93
RDSTL	58.60	59.93	63.13
S-Low	55.87	59.47	64.47
KMM-Soft	56.27	61.20	78.27
KMM-Hard	57.47	60.33	78.47
MLS-Soft	56.27	59.40	77.93
MLS-Hard	57.27	60.40	78.13
GASTL-SoftA	56.67	61.93	78.20
GASTL-HardA	57.87	62.73	78.53
GASTL-SoftB	56.67	62.00	78.20
GASTL-HardB	58.67	61.93	78.60

TABLE 7

Performance of GASTL and competing feature selection algorithms in classification on ESC-50. Classification accuracy (%) is used as the evaluation metric.

Method \ Set ID	1	2	3	4	5
Target Only	20.50	25.00	20.00	19.00	20.00
STL	19.00	19.00	16.00	18.00	20.50
RDSTL	26.00	28.00	25.50	26.50	26.50
S-Low	17.00	15.50	16.00	17.50	15.00
KMM-Soft	21.00	28.00	20.00	22.00	25.00
KMM-Hard	24.00	28.50	23.00	22.00	20.00
MLS-Soft	22.50	26.00	21.00	19.50	25.00
MLS-Hard	23.00	27.50	22.50	22.50	22.00
GASTL-SoftA	26.00	27.50	23.00	23.00	26.00
GASTL-HardA	26.00	30.50	23.50	24.50	24.50
GASTL-SoftB	26.50	28.00	23.50	23.50	26.50
GASTL-HardB	26.00	29.50	24.50	25.00	24.50

in data reconstruction and pseudo-labeling. In order to measure the effect of local data structure preservation on knowledge transfer, we compare the classification performance when $\gamma = 0$ with the optimal one. In Fig. 2, the comparisons on one set of Caltech101 with both SIFTBOW and VGG19 as the input to autoencoder, both IMDB and Twitter with each target data having 10 training samples, and one set of ESC-50 are displayed. We can find that in most cases setting $\gamma = 0$ cannot achieve the optimal performance. Exceptions appear in the cases of “HardA” on Caltech101 with SIFTBOW features and both “HardA” and “HardB” on Twitter. Due to our observations on complete comparisons, classification rates resulted from the situation of $\gamma = 0$ are consistently lower than those resulted from the situations of $\gamma \neq 0$. Therefore, the former exception can be regarded as a subtle outlier. However, we found that the advantages in classification accuracy contributed by local data structure preservation are not obvious on Twitter. One possible explanation is that the local data structures in the space of WORD2VEC feature cannot provide discriminative information for samples in Twitter dataset. Therefore, local data structure preservation negatively affected the knowledge transfer performance reflected by classification accuracy on unlabeled target samples.

4.5.2 The Effect of Source Sample Selection

We claim that transferring knowledge from source samples indiscriminately may cause negative transfer since there

is no guarantee that all source samples have sufficient relevance with target domain. In order to demonstrate the advantages of source sample selection, we compare the classification accuracy for three different cases: the optimal value of p found with GASTL, $p = 0$ (i.e., no transfer learning), and $p = n_{src}$ (i.e., no sample selection). The results shown in Fig. 3 demonstrate not only that significant performance gains are obtained via GASTL, but also that in many cases the blind consideration of all source samples can in fact result in negative transfer, as seen by the reduced performance obtained with $p = n_{src}$ versus $p = 0$.

5 CONCLUSION

In this paper, we propose a graph and autoencoder based self-taught learning (GASTL) method. The main innovations in our self-taught learning methodology with respect to the literature can be summarized as (a) leveraging relevance metrics to select a subset of source samples in transfer learning; (b) considering cross domain relevance for classifier training; and (c) developing our method for hard as well as soft classification problems. With our proposed framework, we decrease negative transfer and improve knowledge transfer performance in many scenarios. Experimental results demonstrate the advantages of GASTL versus methods in the literature.

Our work can be easily extended from a single-layer autoencoder-based design to one based on deep neural networks. We also plan to integrate discriminative information of target samples into our framework.

6 ACKNOWLEDGEMENT

We thank Dr. Sheng Li for providing the code of paper [20].

REFERENCES

- [1] T. G. Dietterich, “Approximate Statistical Tests for Comparing Supervised Classification Learning Algorithms,” *Neural Comput.*, vol. 10, no. 7, pp. 1895–1923, 1998.
- [2] L. O. Jimenez and D. A. Landgrebe, “Supervised Classification in High-Dimensional Space: Geometrical, Statistical, and Asymptotical Properties of Multivariate Data,” *IEEE Trans. Syst. Man Cybern. C Appl. Rev.*, vol. 28, no. 1, pp. 39–54, 1998.
- [3] J. Cohen, P. Cohen, S. G. West, and L. S. Aiken, *Applied Multiple Regression/Correlation Analysis for the Behavioral Sciences*. Routledge, 2013.
- [4] N. R. Draper and H. Smith, *Applied Regression Analysis*. John Wiley & Sons, 2014.
- [5] O. Russakovsky, J. Deng, H. Su, J. Krause, S. Satheesh, S. Ma, Z. Huang, A. Karpathy, A. Khosla, M. Bernstein et al., “Imagenet Large Scale Visual Recognition Challenge,” *Int. J. Comput. Vis.*, vol. 115, no. 3, pp. 211–252, 2015.
- [6] A. Rozantsev, M. Salzmann, and P. Fua, “Beyond Sharing Weights for Deep Domain Adaptation,” *IEEE Trans. Pattern Anal. Mach. Intell.*, DOI: 10.1109/TPAMI.2018.2814042 2018.
- [7] X. Zhu and X. Wu, “Class Noise Handling for Effective Cost-Sensitive Learning by Cost-Guided Iterative

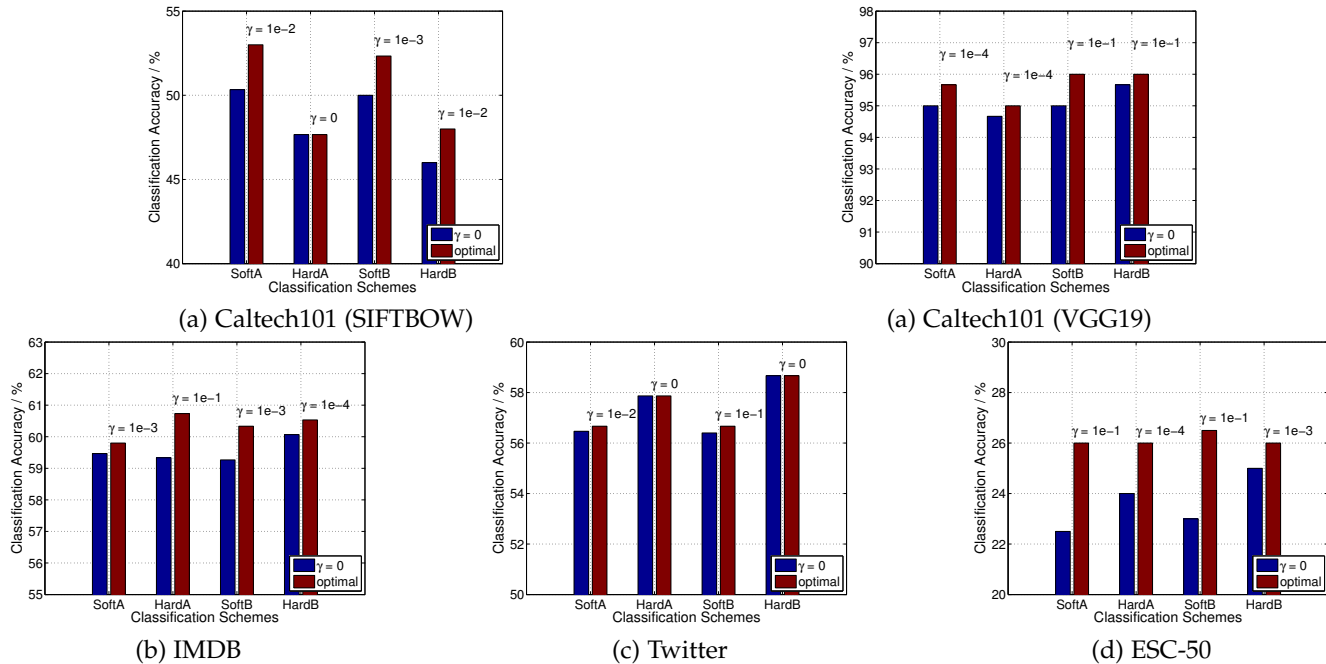


Fig. 2. Comparison of GASTL performance when $\gamma = 0$ and optimal GASTL performance. Classification accuracy (%) is used as the evaluation metric. Optimal values for γ are shown.

- Classification Filtering," *IEEE Trans. Knowl. Data Eng.*, vol. 18, no. 10, pp. 1435–1440, 2006.
- [8] Q. Yang, C. Ling, X. Chai, and R. Pan, "Test-cost sensitive classification on data with missing values," *IEEE Trans. Knowl. Data Eng.*, vol. 18, no. 5, pp. 626–638, 2006.
- [9] K. Nigam, A. K. McCallum, S. Thrun, and T. Mitchell, "Text Classification from Labeled and Unlabeled Documents Using EM," *Mach. Learn.*, vol. 39, no. 2–3, pp. 103–134, 2000.
- [10] S. J. Pan and Q. Yang, "A Survey on Transfer Learning," *IEEE Trans. Knowl. Data Eng.*, vol. 22, no. 10, pp. 1345–1359, 2010.
- [11] K. Weiss, T. M. Khoshgoftaar, and D. Wang, "A Survey of Transfer Learning," *J. Big Data*, vol. 3, no. 1, pp. 1–40, 2016.
- [12] R. Raina, A. Battle, H. Lee, B. Packer, and A. Y. Ng, "Self-Taught Learning: Transfer Learning from Unlabeled Data," in *Int. Conf. Mach. Learn.*, 2007, pp. 759–766.
- [13] W. Dai, Q. Yang, G.-R. Xue, and Y. Yu, "Self-Taught Clustering," in *Int. Conf. Mach. Learn.*, 2008, pp. 200–207.
- [14] J. Kuen, K. M. Lim, and C. P. Lee, "Self-Taught Learning of a Deep Invariant Representation for Visual Tracking via Temporal Slowness Principle," *Pattern Recognit.*, vol. 48, no. 10, pp. 2964–2982, 2015.
- [15] L. Bazzani, A. Bergamo, D. Anguelov, and L. Torrensani, "Self-Taught Object Localization with Deep Networks," in *IEEE Winter Conf. Appl. Comput. Vis.*, 2016, pp. 1–9.
- [16] Z. Jie, Y. Wei, X. Jin, J. Feng, and W. Liu, "Deep Self-Taught Learning for Weakly Supervised Object Localization," *arXiv preprint arXiv:1704.05188*, 2017.
- [17] R. Kemker and C. Kanan, "Self-taught feature learning for hyperspectral image classification," *IEEE Trans. Geosci. Remote Sens.*, vol. 55, no. 5, pp. 2693–2705, 2017.
- [18] P. He, P. Jia, S. Qiao, and S. Duan, "Self-taught learning based on sparse autoencoder for e-nose in wound infection detection," *Sensors*, vol. 17, no. 10, p. 2279, 2017.
- [19] H. Wang, F. Nie, and H. Huang, "Robust and Discriminative Self-Taught Learning," in *Int. Conf. Mach. Learn.*, 2013, pp. 298–306.
- [20] S. Li, K. Li, and Y. Fu, "Self-Taught Low-Rank Coding for Visual Learning," *IEEE Trans. Neural. Netw. Learn. Syst.*, vol. 29, no. 3, pp. 645–656, 2018.
- [21] J. Schmidhuber, "Deep Learning in Neural Networks: An Overview," *Neural Netw.*, vol. 61, pp. 85–117, 2015.
- [22] M. Shao, D. Kit, and Y. Fu, "Generalized Transfer Subspace Learning through Low-Rank Constraint," *Int. J. Comput. Vis.*, vol. 109, no. 1–2, pp. 74–93, 2014.
- [23] D. Cai, C. Zhang, and X. He, "Unsupervised feature selection for multi-cluster data," in *ACM Int. Conf. Knowl. Dis. Data Mining*, 2010, pp. 333–342.
- [24] Q. V. Le, J. Ngiam, A. Coates, A. Lahiri, B. Prochnow, and A. Y. Ng, "On Optimization Methods for Deep Learning," in *Int. Conf. Mach. Learn.*, 2011, pp. 265–272.
- [25] D. C. Liu and J. Nocedal, "On the limited memory BFGS method for large scale optimization," *Math. Program.*, vol. 45, no. 1, pp. 501–528, 1989.
- [26] M. Schmidt, "minFunc: Unconstrained differentiable multivariate optimization in matlab," Available at: <http://www.cs.ubc.ca/~schmidtm/Software/minFunc.html>, 2005.
- [27] C. Hou, F. Nie, X. Li, D. Yi, and Y. Wu, "Joint embedding learning and sparse regression: A framework for unsupervised feature selection," *IEEE Trans. Cybern.*, vol. 44, no. 6, pp. 793–804, 2014.
- [28] Y. Guo, G. Ding, J. Han, and Y. Gao, "Zero-Shot Learning with Transferred Samples," *IEEE Trans. Image Proc.*,

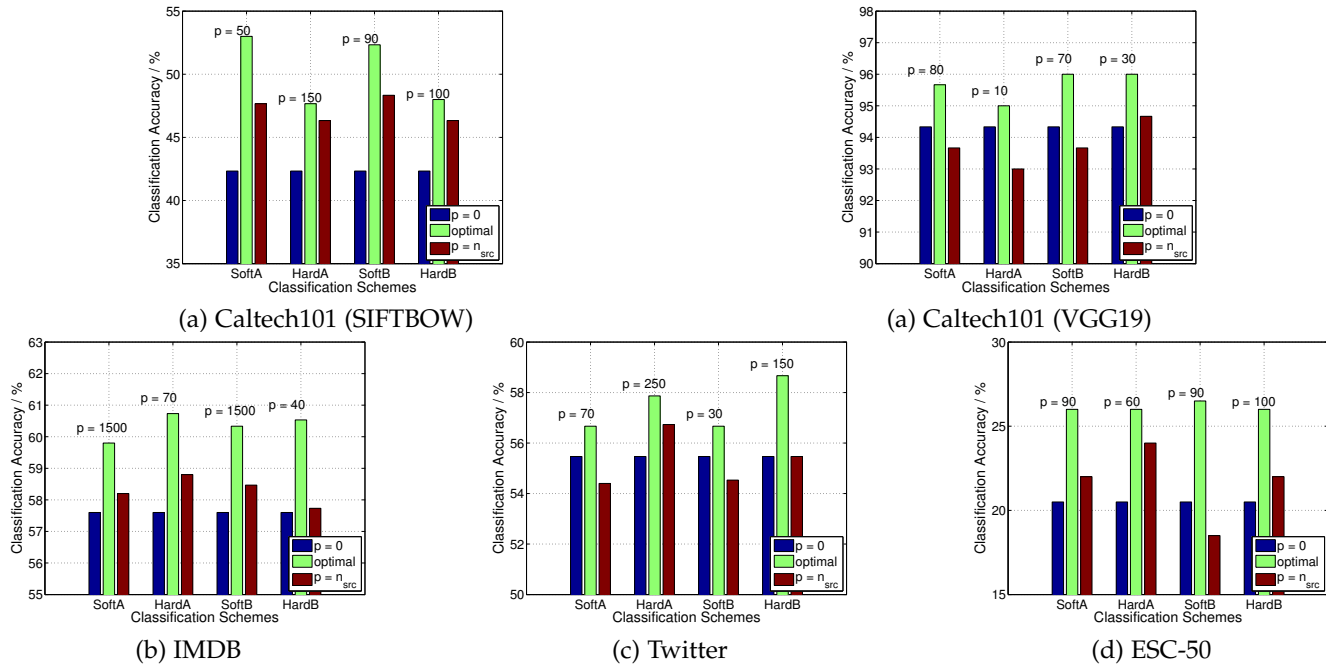


Fig. 3. Comparison of GASTL performance when all source samples are used for classifier training and optimal GASTL performance. Classification accuracy (%) is used as the evaluation metric. Optimal values for p are shown.

vol. 26, no. 7, pp. 3277–3290, 2017.

- [29] R. Socher, M. Ganjoo, C. D. Manning, and A. Ng, “Zero-shot Learning through Cross-Modal Transfer,” in *Adv. Neural Inf. Proc. Syst.*, 2013, pp. 935–943.
- [30] P. Gehler and S. Nowozin, “On Feature Combination for Multiclass Object Classification,” in *IEEE Int. Conf. Comput. Vis.*, 2009, pp. 221–228.
- [31] K. Simonyan and A. Zisserman, “Very Deep Convolutional Networks for Large-Scale Image Recognition,” *arXiv preprint arXiv:1409.1556*, 2014.
- [32] Y. Kim, “Convolutional Neural Networks for Sentence Classification,” in *Conf. Empir. Methods Nat. Lang. Process.*, 2014, pp. 1746–1751.
- [33] K. J. Piczak, “ESC: Dataset for Environmental Sound Classification,” in *ACM Int. Conf. Multimedia*, 2015, pp. 1015–1018.
- [34] B. McFee, C. Raffel, D. Liang, D. P. Ellis, M. McVicar, E. Battenberg, and O. Nieto, “librosa 0.6.1,” <http://dx.doi.org/10.5281/zenodo.1252297>, May 2018.
- [35] J. Huang, A. Gretton, K. M. Borgwardt, B. Schölkopf, and A. J. Smola, “Correcting sample selection bias by unlabeled data,” in *Adv. Neural Inf. Process. Syst.*, 2007, pp. 601–608.
- [36] R. Aljundi, R. Emonet, D. Muselet, and M. Sebban, “Landmarks-Based Kernelized Subspace Alignment for Unsupervised Domain Adaptation,” in *IEEE Conf. Comp. Vis. and Pattern Recognit.*, 2015, pp. 56–63.